Ground-based solar astrometric measurements during the PICARD mission

Irbah A. [a] Meftah M.[a] Corbard T.[b] Ikhlef R.[d] Morand F.[b] Assus P.[b] Fodil M.[d] Lin M.[a] Ducourt E. [a] Lesueur P. [a] Poiet G. [a] Renaud C.[b] and Rouze M.[e]

[a] Université Versailles St-Quentin; CNRS/INSU, LATMOS-IPSL, Guyancourt, France

[b] Université de Nice Sophia Antipolis, CNRS, Observatoire de la Côte d'Azur, BP 4229 06304 Nice Cedex 4, France

[c] Université de Nice-Sophia Antipolis, UMR 6525 Astrophysique, Parc Valrose F-06108 Nice Cedex 2, France

[d] CRAAG - Observatoire d'Alger BP 63 Bouzaréah Alger, Algérie

[e] Centre National d'Etudes Spatiales - CNES - Toulouse 31401, France

ABSTRACT

PICARD is a space mission developed mainly to study the geometry of the Sun. The satellite was launched in June 2010. The PICARD mission has a ground program which is based at the Calern Observatory (Observatoire de la Côte d'Azur). It will allow recording simultaneous solar images from ground. Astrometric observations of the Sun using ground-based telescopes need however an accurate modelling of optical effects induced by atmospheric turbulence. Previous works have revealed a dependence of the Sun radius measurements with the observation conditions (Fried's parameter, atmospheric correlation time(s) ...). The ground instruments consist mainly in SODISM II, replica of the PICARD space instrument and MISOLFA, a generalized daytime seeing monitor. They are complemented by standard sun-photometers and a pyranometer for estimating a global sky quality index. MISOLFA is founded on the observation of Angle-of-Arrival (AA) fluctuations and allows us to analyze atmospheric turbulence optical effects on measurements performed by SODISM II. It gives estimations of the coherence parameters characterizing wave-fronts degraded by the atmospheric turbulence (Fried's parameter, size of the isoplanatic patch, the spatial coherence outer scale and atmospheric correlation times). This paper presents an overview of the ground based instruments of PICARD and some results obtained from observations performed at Calern observatory in 2011.

Keywords: Atmospheric turbulence, seeing monitor, Sun

1. INTRODUCTION

The PICARD space mission[1] was launched in June 15, 2010 mainly for studying the geometry of the Sun and its evolution with the solar cycle. PICARD has also a ground segment program to allow observations from the ground. In fact, solar diameter measurements performed at Calern Observatory (Observatoire de la Côte d'Azur) during many years have shown long-time variations,[2,3] which are not still well explained. Are they due to the Sun or to the Earth atmosphere ? A previous diameter measurement analysis revealed a dependence with seeing conditions as represented by Fried's parameter r_0.[4] Numerical simulations were then developed in order to better understand atmospheric effects on diameter measurements with a specific instrument.[5] The results showed a decrease of the error with the seeing but strongly conditioned with the turbulence coherence times. The error has also a weak dependence with the outer scale $\mathcal{L}_0$ for small aperture telescopes. A seeing monitor is then useful for this kind of solar measurements and MISOLFA was built for this goal. It is a generalized daytime seeing monitor founded on observations of Angle-of-Arrival (AA) fluctuations (solar limb image motion) and their

Further author information:
Send correspondence to Irbah Abdanour - E-mail: air@latmos.ipsl.fr - Telephone: +33 (0)180 285 040

statistical analysis. MISOLFA gives estimations of the coherence parameters characterizing wave-fronts degraded by atmospheric turbulence (Fried's parameter r_0, size of the isoplanatic patch θ_0, spatial coherence outer scale $\mathcal{L}_0$ and atmospheric correlation times). The monitor will also give access to optical turbulence profiles.[6] MISOLFA observe now together with the qualification model of the PICARD space instrument which is delivering its data since July 2010. The qualification model instrument begun to observe at Calern Observatory since March 2011. The main objectives are the comparison of the results deduced from space and ground data as well as the evaluation of the atmospheric turbulence optical effects on the measurements performed from the ground. Simultaneous ground measurements at Calern with the the qualification model instrument and the solar seeing monitor MISOLFA will help calibrating the atmospheric distortion of the data for both astrometric and imaging techniques. A continuation of ground-based series would then allow to detect possible long-time variations of the global geometry of the Sun. We present first in this paper the PICARD ground-based instruments and give after that some results obtained from the observations at the Calern observatory.

2. THE GROUND-BASED INSTRUMENTS OF THE PICARD MISSION

PICARD is a satellite dedicated to the simultaneous measurement of the solar diameter, the solar shape, the solar irradiance and the solar interior.[1] The PICARD payload consists in absolute radiometers and photometers measuring the total solar irradiance and in the SODISM instrument which is an imaging telescope developed to determine the diameter, the limb shape and the asphericity of the Sun. The PICARD mission has also a ground segment consisting of several instruments based at the Calern observatory. The ground segment is composed with the qualification model of the space instrument, MISOLFA the solar seeing monitor and some others ground-based instruments giving useful data such as the solar irradiance, air temperatures, the wind velocity and directions, the nebulosity etc. Figure 1 shows the PICARD ground-based instruments installed at the Calern observatory. We will focus here mainly around the SODISM instrument and its qualification model and on the solar seeing monitor MISOLFA.

Figure 1. Overview of the instruments of the PICARD ground segment : SODISM II is in the foreground of the image while MISOLFA is in the background.

2.1 The PICARD space instrument and its qualification model

2.1.1 The PICARD space instrument

A full description of the PICARD space instrument can be found in Meftah *et al.*[7] and we recall here only its main properties. SODISM (Solar Diameter Imager and Surface Mapper) is an 11-cm diameter Cassegrain telescope associated with a 2048x2048 pixels CCD detector where the whole SUN is formed. Wavelengths are selected by mean of interference filters placed on 2 wheels. Wavelength domains have been chosen free of Fraunhofer lines (535.7, 607.1 and 782.2 nm). Active regions are detected in the 215 nm domain and the CaII (393.37 nm) line. Helioseismologic observations are performed at 535.7 nm.[8] The satellite platform is stabilized within 36

arcseconds filed. The telescope primary mirror stabilizes then the Sun image within 0.2 arc-second using piezo electric actuators. An internal calibration system composed with 4 prisms, allows to follow scale factor variations induced by instrument deformations resulting from temperature fluctuations in orbit or others causes.[9] This is obtained by processing the 4 corner images formed at 535 nm by the prisms. The diameter measurements are referred to star angular distances by rotating the spacecraft towards some doublet stars several times per year. The instrument stability is assured by use of stable materials (Zerodur for mirrors, Carbon-Carbon and Invar for structure). The whole instrument is temperature stabilized within 1^{o}C. The CCD is also temperature stabilized around -7^{o}C within 0.2^{o}C. In order to limit the solar energy, a window is set at the telescope entrance limiting the input to 5% of the total solar irradiance. No significant ageing has been measured in laboratory for all the duration of the mission. The optical scheme of SODISM is shown in Figure 2.

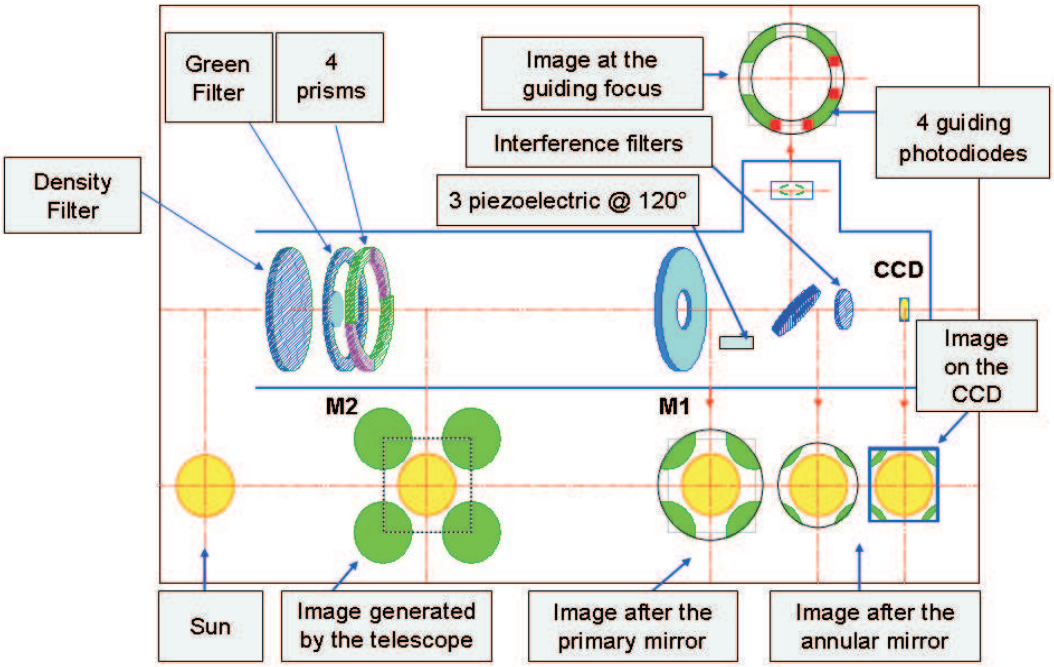

Figure 2. SODISM optical scheme.

2.1.2 SODISM II, the qualification model

The SODISM qualification model named SODISM II was installed at the Calern Observatory in March 2011 and record solar images since this date. Some adaptations were required before installing the instrument on the site. SODISM II was placed first in a vacuum tank deporting by the way the entrance windows at its front. The whole system SODISM II and tank were installed on an equatorial mount to follow the Sun. The 215 nm filter was replaced with another one centered around 1025 nm. Since the instrument as well as the flight software were similar to the space ones, a satellite simulator was needed to access and control SODISM II. A special acquisition and processing system was then developed to send program plans to the instrument for acquiring data and consequently to build all SODISM II L0 products from incoming data packets as done with the PICARD payload data center[10] situated at Brussels (Belgium). Some additional housekeeping data were also defined and recorded such as all weather data (temperature, wind velocity and directions etc.), guiding system and SODISM II environment parameters. These data are all added to L0 product headers of SODISM II. The helioseismologic program have been removed from ground but solar images are however recorded with the corresponding filter for the objectives of solar diameter measurements. Doublet stars are also regularly recorded to estimate the absolute scale factor while the corner images at 535 nm used to follow diurnal and long-terme variations of the internal one.

2.2 The solar seeing monitor MISOLFA

We recall here the main properties of the solar monitor MISOLFA (*Moniteur d'Images SOLaires Franco-Algérien*) since more details may be found in irbah *et al.*[11] The objectives of MISOLFA are to evaluate and model atmospheric turbulence optical effects on measurements performed from the ground. MISOLFA measures the integrated optical parameters (Fried's parameter r_0, the spatial coherence outer scale $\mathcal{L}_0$, the size of isoplanatic patch θ_0 and the correlation time(s) of the fluctuations τ_0) in the framework of a turbulent model (the Von Kàrmàn model for example). It gives also access to the vertical profile of the optical turbulence which correponds to the structure constant of the air refractive index fluctuations $C_n^2(h)$. The MISOLFA principle is based on the statistical analysis of AA-fluctuations. The AA-fluctuations, which are fluctuations of the normal to the perturbed wavefronts, can be directly observed in the image plane (this is the case of Shack-Hartmann's sensors currently used in the adaptive optics systems). They may be also observed in the pupil plane when the astronomical sources present an intensity distribution with a strong discontinuity (for example the Sun or the Moon).[12] In this case, an analysis of the perturbed wavefronts analog to a Foucault test can be performed.[13] Figure 3 shows the principle of the monitor experimental device. It consists in 2 ways. The first one named in the following *image plane observation way*, allows recording directly the AA-fluctuations using a CCD camera placed on the solar limb image (N^{o}1). The entrance window is chosen prismatic to form two solar limb images on the CCD at the same time : a direct image and a reflected one due to an internal reflection beam inside the entrance window. The reflected image of the solar limb is the opposite part of the direct one. A beam splitter allows to create a second way named in the following *pupil plane observation way* in which the telescope pupil (P1) is observed by means of a lens through a narrow slit placed on the solar limb image (N^{o}2). The diaphragm size is some arc-seconds wide and about fifty arc-seconds length. The pupil image intensity presents fluctuations which are proportional to the AA-fluctuations. Several photodiodes allow recording the intensity fluctuations with optical fibers positioned on the image behind diaphragms of different sizes. The signals given by the different photodiodes will be simultaneously recorded and a spatiotemporal analysis performed.

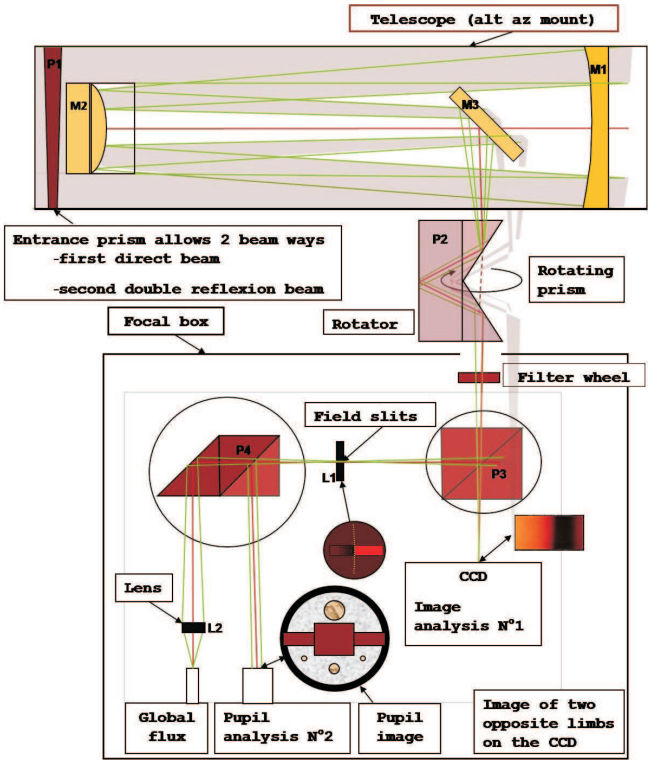

Figure 3. MISOLFA : experimental device.

2.2.1 The image plane observation way

The transverse angular covariance of AA-fluctuations observed with a telescope in 2 directions separated by θ, is expressed in the case where the atmospheric turbulence is described by the Von Kàrmàn model as:[11]

$$\mathcal{C}_\alpha(\theta) \quad = \quad 0.0716\lambda^2 r_0^{-\frac{5}{3}} \int_0^{+\infty} df f^3 (f^2 + \frac{1}{{\mathcal{L}_0}^2})^{-\frac{11}{6}} [J_0(2\pi f\theta h) + J_2(2\pi f\theta h)][\frac{2J_1(\pi Df)}{\pi Df}]^2 \tag{1}$$

where f is an angular frequency, D the telescope pupil, λ the wavelength and J_0, J_1, J_2 the Bessel functions of the first kind. The spatial coherence inner scale is taken equal to 0 in the Von Kàrmàn model.
Using inversion techniques, Equation 1 allows estimating the Fried parameter r_0, the spatial coherence outer scale $\mathcal{L}_0$ and the isoplanatic angle θ_0 deduced from the ratio r_0/h. h is the altitude of an equivalent impulse layer giving same optical effects at ground level than the whole turbulent terrestrial atmosphere.
In the case of a multilayer turbulent atmosphere, we use also Equation 1 with the same assumptions to deduce :

$$\mathcal{C}_\alpha(\theta) = 1.19 \int_0^{+\infty} dh C_n^2(h) \int_0^{+\infty} df f^3 (f^2 + \frac{1}{L_0(h)^2})^{-\frac{11}{6}} [J_0(2\pi f\theta h) + J_2(2\pi f\theta h)][\frac{2J_1(\pi Df)}{\pi Df}]^2 \tag{2}$$

where $C_n^2(h)$ is the energy vertical profile of the " optical " turbulence given by the structure constant for the air refractive index fluctuations. $L_0(h)$ is the turbulent outer scale vertical profile.
The transverse angular structure function is given by :

$$d_\alpha(\theta) = 2[\sigma_\alpha^2 - \mathcal{C}_\alpha(\theta)] \tag{3}$$

where $\sigma_\alpha^2 = C_\alpha(0)$. Introducing (3) in Equation (4) leads to :

$$d_\alpha(\theta) = 2.4 \int_0^{+\infty} dh C_n^2(h) \int_0^{+\infty} df f^3 (f^2 + \frac{1}{L_0(h)^2})^{-\frac{11}{6}} [1 - J_0(2\pi f\theta h) - J_2(2\pi f\theta h)][\frac{2J_1(\pi Df)}{\pi Df}]^2 \tag{4}$$

As a first approach we can consider the case in which $L_0(h) = \infty$ for which the optical turbulence profile $C_n^2(h)$ can be estimated by application of the inversion technique described in Bouzid *et al.*[6]

2.2.2 The pupil-plane observation way

Evolution characteristic times of AA-fluctuations will be estimated using the pupil-plane observation way thanks to its high acquisition rate. Light rays of the atmospheric perturbed wavefront undergo random angles and pass or not through the diaphragm. The pupil illumination observed through the diaphragm will be then related to the local slopes of the wave-front. Intensity variations in the pupil-plane image are therefore directly related to AA-fluctuations at the telescope entrance pupil when an incoherent extended source is observed. The intensity fluctuations is the summation over the angular field-of-view allowed by the optical system (i.e. the diaphragm angular size) of all intensity contributions of point sources situated in $\overrightarrow{\alpha_0}$ angular directions:

$$I(\overrightarrow{r}) = \int d\overrightarrow{\alpha_0} I_{\overrightarrow{\alpha_0}}(\overrightarrow{r}) \propto \int d\overrightarrow{\alpha_0} G_s(\overrightarrow{\alpha_0}) |FT^{-1}[G_s(\overrightarrow{\alpha}) FT[P(\overrightarrow{r}) \sqrt{I_0(\overrightarrow{\alpha_0})} \psi_{\overrightarrow{\alpha_0}}(\overrightarrow{r}) \exp(\frac{2\pi i}{\lambda} \overrightarrow{\alpha_0}\overrightarrow{r})]]|^2 \tag{5}$$

where $\overrightarrow{r(x,y)}$ is a space vector in the pupil-plane, λ the wavelength and $G_s(\overrightarrow{\alpha})$ the diaphragm angular transmission. $P(\overrightarrow{r})$ is the pupil function equal to one inside the pupil area and to zero outside. $I_0(\overrightarrow{\alpha_0})$ and $\psi_{\overrightarrow{\alpha_0}}(\overrightarrow{r})$ are respectively the angular intensity distribution and the normalized turbulence-disturbed complex amplitude of a monochromatic wave expressed at the ground level as $\sqrt{I_0(\overrightarrow{\alpha_0})}\psi_{\overrightarrow{\alpha_0}}(\overrightarrow{r}) \exp(\frac{2\pi i}{\lambda}\overrightarrow{\alpha_0}\overrightarrow{r})$.
Equation 5 is the basic mathematical model giving the intensity fluctuations in the pupil-image of an incoherent extended object. If the considered object is the solar limb assuming by the way that its intensity has a linear relationship with $|\overrightarrow{\alpha}|$ along the diaphragm length positioned following the x-direction in the instrument focal plane, Equation 5 leads to:[16]

$$I(\overrightarrow{r}) \propto P(\overrightarrow{r}) \frac{\partial \varphi(\overrightarrow{r}(x,y))}{\partial y} \tag{6}$$

where $\propto$ denotes the proportionality operator and $\varphi(\overrightarrow{r})$ is the perturbed wave-front phase at the telescope entrance pupil. The phase derivative fluctuations at each wave-front point correspond to AA-fluctuations. The pupil-image observation way introduce a spatial filtering in the image due to the diaphragm leading to measure AA-fluctuations in the y-direction. Berdja *et al.*[13] have shown the good linear relationship between AA-fluctuations and intensity fluctuations as modeled with Equation 6 when the solar limb is observed.
The spatial coherence parameters r_0 and $\mathcal{L}_0$ may be obtained with the pupil-plane observation way together with AA fluctuation characteristic times. The structure function of AA-fluctuations recorded by mean of a pair of photodiodes positioned in the pupil image may be expressed as:[14]

$$d_\alpha(s) = 0.364[1 - k(\frac{s}{D_p})^{-\frac{5}{3}}]\lambda^2 {r_0}^{-\frac{5}{3}} {D_p}^{-\frac{5}{3}} \tag{7}$$

where k is a constant respectively equal to 0.541 or 0.810 according that we consider AA projected on the baseline formed by the photodiodes separated by the distance s or onto a perpendicular direction. D_p is the area integration size of the photodiodes. Equation 7 will be used to calculate r_0.
The spatial coherence outer scale $\mathcal{L}_0$ may be deduced from Equation 1 for θ equal 0. The integration gives in this case and considering that $\mathcal{L}_0$ is great in regard to D_p:[15]

$$\mathcal{C}_\alpha(0, D_p) = 0.017\lambda^2 {r_0}^{-\frac{5}{3}}[{D_p}^{-\frac{1}{3}} - 1.525{\mathcal{L}_0}^{-\frac{1}{3}}] \tag{8}$$

The $\mathcal{L}_0$ parameter will be obtained from Equation 8 applied to 2 photodiodes of different area integration sizes D_{p1} and D_{p2}. It will be obtained from the ratio $r_{\mathcal{L}_0}$:

$$r_{\mathcal{L}_0} = \frac{\mathcal{C}_\alpha(0, D_{p1}) - \mathcal{C}_\alpha(0, D_{p2})}{\mathcal{C}_\alpha(0, D_{p1})} = \frac{{D_{p1}}^{-\frac{1}{3}} - {D_{p2}}^{-\frac{1}{3}}}{{D_{p1}}^{-\frac{1}{3}} - 1.525{\mathcal{L}_0}^{-\frac{1}{3}}} \tag{9}$$

3. SOME FIRST RESULTS

This section presents some results obtained from an analysis of solar data recorded with the PICARD ground-based instruments. The considered data were recorded with MISOLFA and SODISM II observing together at the Calern observatory .

3.1 MISOLFA image analysis and calibration data

Data were recorded with MISOLFA using its two observation way devices (see section 2.2). Data incoming from the *image plane observation way* consist in image series of about 2400 samples recorded at a rate of 30 images per seconds.[11] Figure 4 shows an image of the Sun recorded August 11, 2011 with this observation way. Their

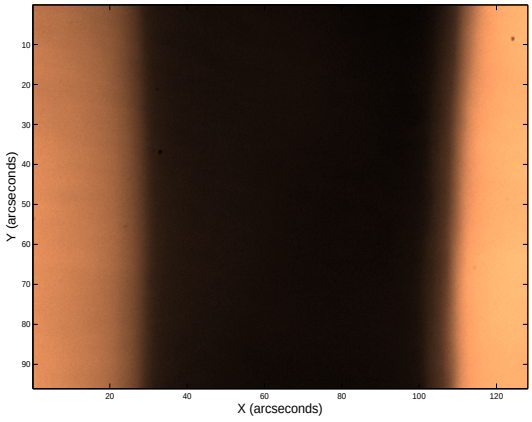

Figure 4. A solar image obtained with the image-plane observation way of MISOLFA.

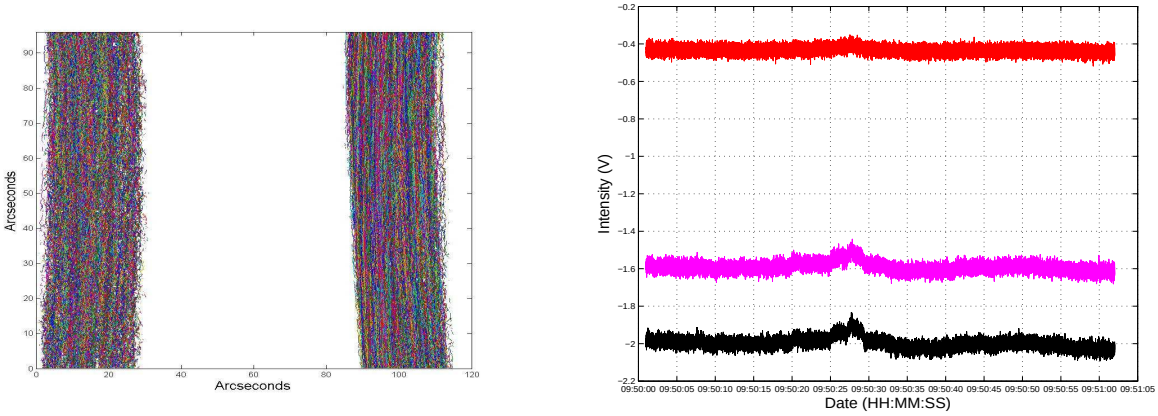

Figure 5. Extracted limbs from images (left side) and intensity fluctuations recorded by the photodiodes (right side)

size is about 96 by 128 arc-seconds. Each CCD pixel line of the direct and reflected limb images is in a direction parallel to the horizon. AA-fluctuations are obtained from temporal series of solar images by extracting their contour (see the left side of figure 5) and then its fluctuations relatively to a mean one. Data of the *pupil plane observation way* come from the 5 photodiodes of different integration areas delivering their output signal at a rate of 1 Kilohertz. The right side of the figure 5 shows intensity fluctuations recorded August 11, 2011 by one photodiode of size 1 millimeter (red curve) and with 2 others of size 2 millimeters (curves in magenta and black). These two last correspond to integration of pupil image areas which sizes are respectively 2 millimeters and 1 centimeter which is the size of the whole pupil image.

3.1.1 Calibration of intensity fluctuations in the pupil plane

The aim with the first available data simultaneously recorded with the 2 observation way devices was then to validate Equation 6. This equation which links intensity fluctuations in the pupil image to AA-fluctuations, will allow too calibrating output voltage of the photodiodes in angle units (commonly in arc-seconds). We use for that the data of the figure 5 (left side) to compute the solar image motion since we intentionally let the telescope having a temporal drift during observations. We then consider the intensity fluctuations of the whole pupil image recorded by the appropriate photodiode. We observe that the corresponding curves have the same trend although their temporal sampling is different (see the left side of figure 6). We are then able to calibrate the intensity

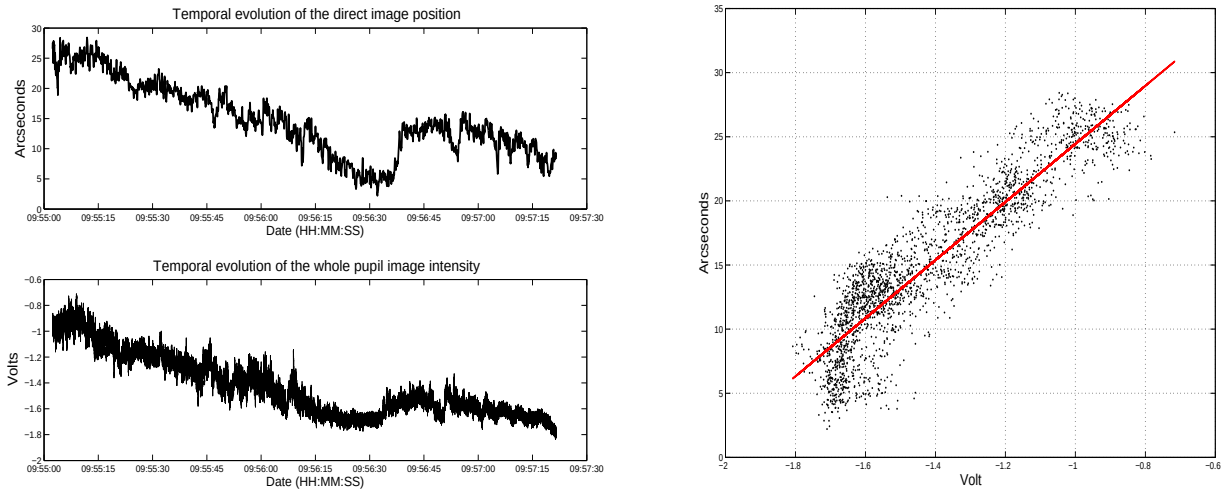

Figure 6. Fluctuations of respectively the solar limb positions in the image plane and the intensity of the whole image of the pupil plane (right side). The left side of the figure shows the relationship between arc-seconds and volts

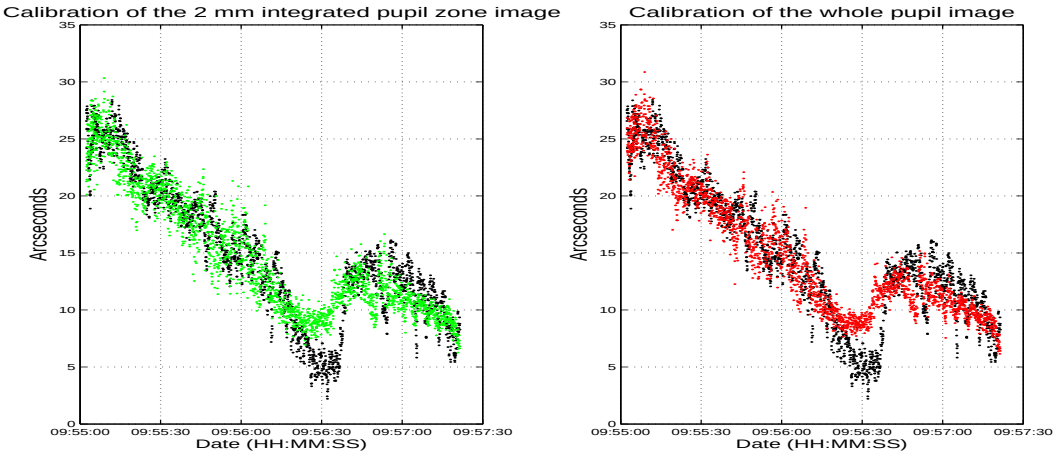

Figure 7. Calibration of the intensity fluctuations in the pupil image.

fluctuations expressed in voltage since we know the spatial sampling in the focal plane (0.2 arc-seconds per pixel). The left side of figure 6 shows the solar image positions versus the intensity fluctuations. A linear relationship is clearly observed between the two variables validating by the way Equation 6. We will use this result to calibrate AA-fluctuations measured in the pupil plane with a high frequency rate thanks to the photodiodes. The figure 7 shows calibrated AA-fluctuations recorded with the photodiodes of size 2 millimeters superimposed with those directly obtained in the focal image with a low frequency rate. The results are consistent and therefore allow us to consider the estimation of spatial turbulence parameters with the pupil plane data as described in section 2.2.2.

3.1.2 Estimation of turbulence parameters with pupil and focal plane data

The same image series used for calibration of intensity fluctuations in the pupil plane (see previous section) were taken to estimate also the spatial turbulence parameters. The experimental covariance function $\mathcal{C}(\theta)$ and then the structure function $d(\theta)$ have been computed using the data of figure 5 (left side). The Fried parameter r_0, the spatial coherence outer scale $\mathcal{L}_0$ and the altitude of the equivalent impulse layer h are then estimated fitting $d(\theta)$ with the theoretical model given by Equation 1 and 3 (see figure 8) as done by irbah *et al.* (2010).[11] The Fried

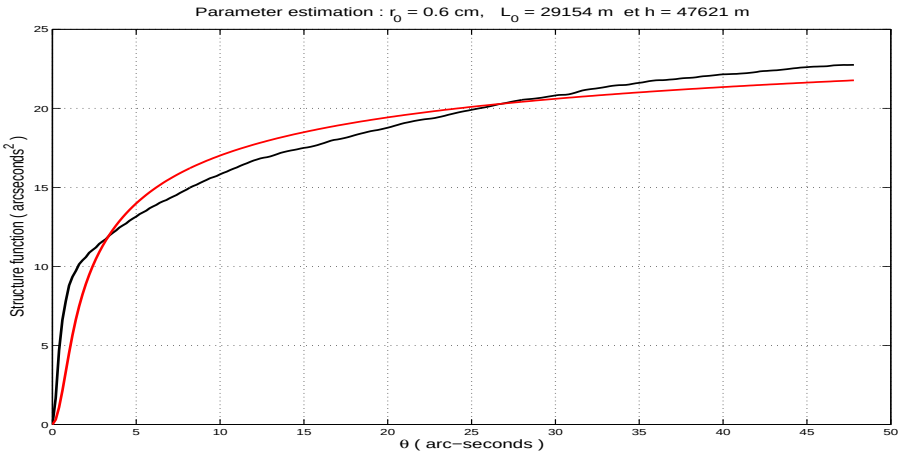

Figure 8. Model fitting to estimate the seeing conditions with solar image series recorded August 11, 2011.

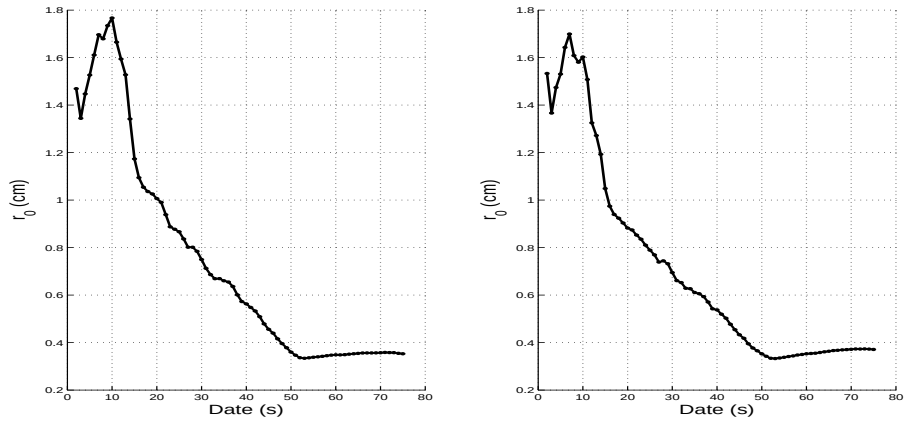

Figure 9. Fried's parameter estimated from direct (right) and reflected (left) solar image series recorded August 11, 2011 considering the shift derivation.

parameter r_0, the spatial coherence outer scale $\mathcal{L}_0$ and the impulse layer altitude h have been found respectively equal to 0.6 cm, 29154 m and 47621 m. We observe that the values found and the fit are of poor quality due to the telescope drift during observations. In addition, we can see that the value of $\mathcal{L}_0$ are large allowing to considerer the Kolmogorov model for r_0 estimation:[4,17]

$$r_0 = 8.25\ 10^5 \lambda^{\frac{6}{5}} D^{-\frac{1}{5}} {\sigma_\alpha}^{-\frac{6}{5}} \tag{10}$$

where the standard deviation σ_α is expressed in arc-seconds in Equation 10. This equation have been used to compute Fried's parameter and the results are shown in figure 9. The standard deviation σ_α of AA-fluctuations is computed considering the fluctuations of the solar limb position of the central line of the direct and reflected image over increasing time intervals up to 74 seconds. We observe that the Fried parameter value has a rapid decrease when the integration time used to compute σ_α exceeds 10 seconds. The final value of r_0 obtained when considering all the series image duration (74 seconds), is of the same order as the one found when fitting the experimental structure function with the theoretical model. We compute in a second case, the standard deviation of the limb position over duration of 2 seconds i.e. we divide the whole temporal signal of limb positions in short samples of equal duration. The result is shown in the figure 10. We observe that we find more realistic values for r_0 with either direct or reflected images. The temporal length of the sample to compute σ_α is an important factor when we want to estimate the turbulence parameter particularly if a telescope drift remains. Finally, we use data of the *pupil plane observation way* to estimate the correlations time of AA-fluctuations.

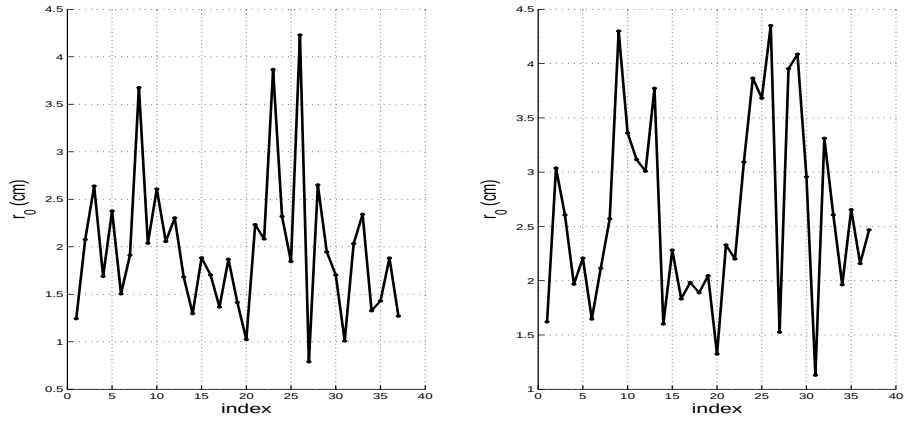

Figure 10. Fried's parameter estimated from direct (right) and reflected (left) solar image series recorded August 11, 2011.

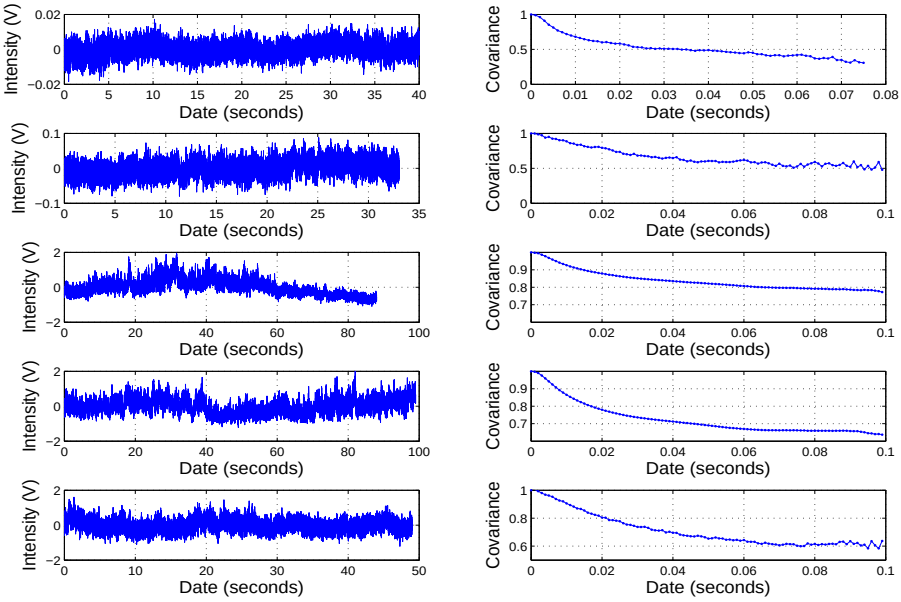

Figure 11. Intensity fluctuations in the pupil image (1 mm photodiode diameter size) and its covariance.

The left side of figure 11 shows from top to bottom some temporal signal of intensity fluctuations recorded June 6 (1 samples), 9 (1 samples), 27 (2 samples) and 28 (1 sample), 2011 at the Calern observatory. The photodiode size is 1 millimeter for all temporal samples and the frequency rate is 1 Kilohertz. the recording time is several tens of seconds for all samples. The covariance function of each sample signal is computed (see the right side of figure 11) and the correlation time deduced. It is defined as the temporal equivalent width giving the same covariance area. Note that it is not necessary to calibrate the intensity fluctuations in angle units before calculating the correlation times. We find respectively 39.02, 65.25, 83.05, 71.87 and 70.29 milliseconds for the 5 AA-fluctuation samples of figure 11 .

3.2 First analysis of solar images recorded with SODISM II

SODISM II records full solar images at several wavelengths at Calern observatory since March, 2011. the objective of acquiring these images is essentially solar diameter measurement. The solar diameter is defined as the position of the inflexion point of the limb darkening function. This function is the intensity variation of the Sun along its radius. The left side of figure 12 shows a solar image recorded August 11, 2011 10:50 UT at

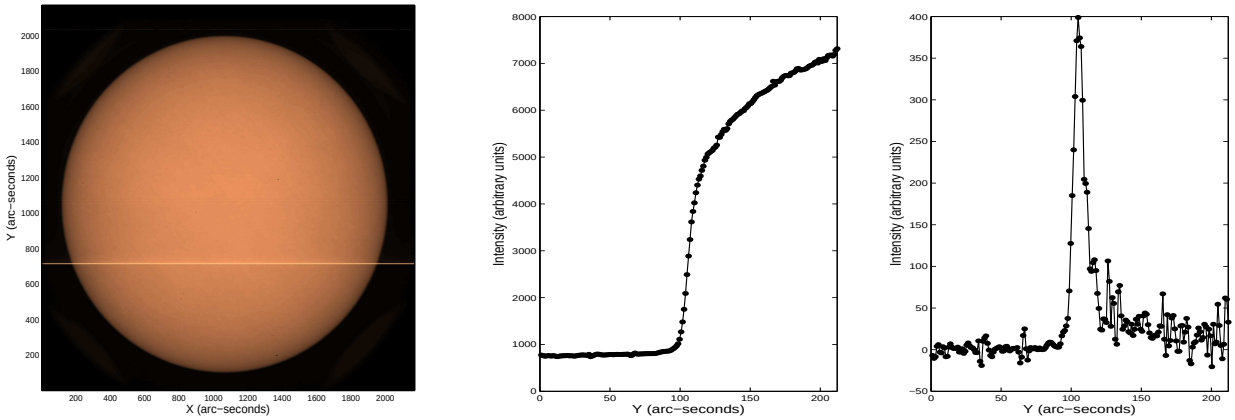

Figure 12. Solar image recorded August 11, 2011 with SODISM II (left). Extracted solar limb and its derivative (right)

535.75 nm. The exposure time was 0.64 second and the image size is 2048x2048 pixels. Each pixel has a size of 1.06 arc-seconds wide. We can see also in the figure, the 4 corner images (see section 2.1.1) as well as some bad CCD lines. The right side of figure 12 shows a part of the limb darkening function near the solar edge. Its first derivative is also shown in the figure. Note that for this image the limb spread over little more than 6 pixels i.e. 6.43 arc-seconds. The left side of figure 13 shows the same solar image and its extracted contour. Each contour point corresponds to the inflexion point position of the limb darkening function in an angular direction in a polar coordinate system. A special filtering was applied to avoid the bad CCD lines. All contour points are then fitted with an ellipse and the solar diameter estimated from the fit parameters. The solar diameter for this image is found equal to 959.719 arc-seconds which is in good agreement with previous measurement values.[3] The right side of figure 13 shows the solar diameter measurements obtained from all the images recorded August 11, 2011 at all SODISM II wavelengths.

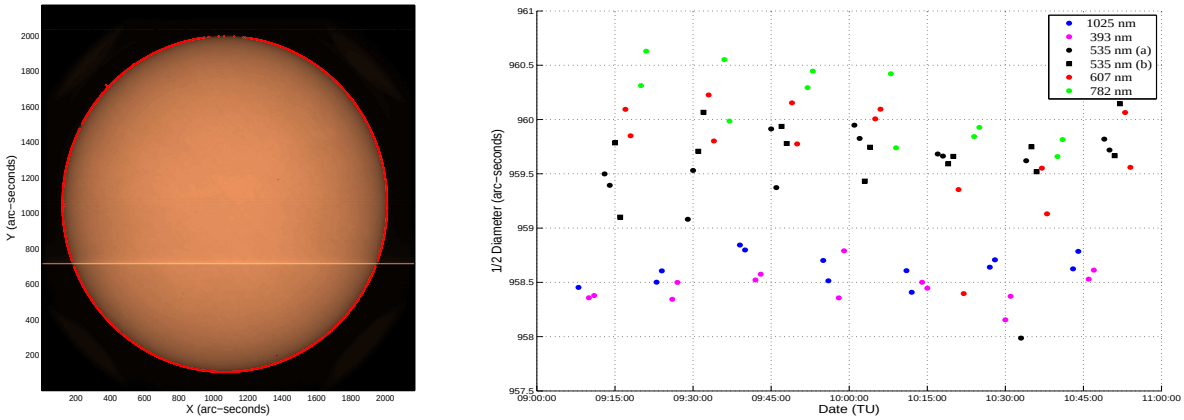

Figure 13. Solar image recorded August 11, 2011 with SODISM II and its estimated contour (left). Solar radius obtained from solar images recorded August 11, 2011 at Calern observatory (right)

4. CONCLUSION

The PICARD satellite was launched June 15, 2010 for solar observations mainly for the diameter measurement of the Sun. In fact, several solar diameter measurement performed at Calern observatory during many years showed variations that are not well explained. Thus SODISM II, the qualification model of the PICARD space instrument was installed at Calern observatory near MISOLFA, a solar seeing monitor. These instruments complemented with standard sun-photometers and a pyranometer for estimating a global sky quality index, compose the ground segment of the PICARD mission. SODISM II and MISOLFA have been presented in this paper as well as some results obtained from observations performed with these instruments. The first results obtained with the two observation way devices of MISOLFA are very promising. We are able to follow *AA*-fluctuations in the pupil plane at a very high frequency rate and estimate their correlation time. Some values for this atmospheric parameter have been given. The first observations with SODISM II are also promising since the first solar diameter measurements are in good agrement with those obtained on the same site with others instruments.

ACKNOWLEDGMENTS

This work has been supported with the support of the Centre National d'Etudes Spatiales (France), the CNRS and the French Foreign Affair Ministry in the framework of the scientific cooperation contract TASSILI 07MDU713 between France and Algeria.

REFERENCES

1. G. Thuillier, S. Dewitte, W. Schmutz and the PICARD team, *Advance Space Research*, 38, 1792, 2006.
2. F. Laclare, C. Delmas, J.P. Coin and A. Irbah,*Solar Phys.*, 166, 211, 1996.

3. F. Morand, C. Delmas, T. Corbard, B. Chauvineau, A. Irbah, M. Fodil and F. Laclare, *Comptes Rendus Physique*, 12, 660, 2011
4. A. Irbah, F. Laclare, J. Borgnino and G. Merlin,*Solar Phys.*, 149, 213, 1994.
5. L. Lakhal, A. Irbah, M. Bouzaria, J. Borgnino, F. Laclare, C. Delmas, *Astron. Astrophys. Suppl. Ser.*, 138, 155, 1999.
6. A. Bouzid, A. Irbah, J. Borgnino J. and H. Lantri H., Marrakech Site 2000, Astronomical Site Evaluation in the Visible and Radio Range, Marrakech - Morocco, November 13-17, 2000.
7. M. Meftah, M. Meissonnier, A. Irbah, S. Abbaki, P. Assus, E. Bertran, J.P. Dubois, E. Ducourt, C. Dufour, J.P. Marcovici, G. Poiet, A.J. Vieau and G. Thuillier, "The space instrument SODISM and the ground instrument SODISM II", Space Telescopes and Instrumentation 2010: Optical, Infrared, and Millimeter Wave. Edited by Oschmann, Jacobus M., Jr.; Clampin, Mark C.; MacEwen, Howard A. Proceedings of the SPIE, Volume 7731, pp. 773145-773145-12, 2010.
8. T. Corbard, P. Boumier,T. Appourchaux, S.J. Jiménez-Reyes, B. Gelly and the PICARD team, *Astron. Nachr.*, 329, No. 5, 508 - 516, 2008.
9. P. Assus, A. Irbah, P. Bourget, T. Corbard and the PICARD team, *Astron. Nachr.*, 329, No. 5, 517 - 520, 2008.
10. G. Pradels, T. Guinle, G. Thuillier, A. Irbah, J.P. Marcovici, D. Moreau, C. Noel and M. Dominique, SPACEOPS conference, 2008
11. A. Irbah , T. Corbard, P. Assus, J. Borgnino, C. Dufour, R. Ikhlef, F. Martin, M. Meftah, F. Morand, C. Renaud and E. Simon , "The solar seeing monitor MISOLFA: presentation and first results", Ground-based and Airborne Instrumentation for Astronomy III. Edited by McLean, Ian S.; Ramsay, Suzanne K.; Takami, Hideki. Proceedings of the SPIE, Vol. 7735, pp. 77356F-77356F-9, 2010
12. A. Irbah, J. Borgnino, F. Laclare, and G. Merlin, "Isoplanatism and high spatial resolution solar imaging," *Astron. Astrophys.*, 276, pp. 663–672, 1993.
13. A. Berdja, A. Irbah , J. Borgnino and F. Martin , "Simulmation of pupil-plane observation of angle-of-arrival fluctuations in daytime turbulence, in Optics in Atmospheric", Propagation and Adaptive Systems VI, edited by John D. Gonglewski and Karin Stein, Proceedings of SPIE Vol. 5237 (SPIE, Bellingham, WA, 2004), p. 238-248, 2004
14. M. Sarazin and F. Roddier, The ESO differential image motion monitor, Astron. and Astrophys., 227, p. 294-300, 1990
15. A. Ziad , J. Borgnino , F. Martin and A. Agabi , "Experimental estimation of the spatial coherence outer scale from a wavefront statistical analysis", Astron. and Astrophys. 282, p. 1021-1033, 1994
16. J. Borgnino, A. Berdja, A. Ziad and J. Maire, "An Optical Turbulence Profiler for the terrestrial atmosphere boundary-layer", Proceedings of Symposium of Seeing, Kona, Hawaii, 20-22 March 2007, T. Cherubini and S. Businger, eds., 2007
17. J. Borgnino, G. Ceppatelli, G. Ricort and A. Righini, Astron. Astrophys. 107, 333, 1982